COMPDYN 2015
5th ECCOMAS Thematic Conference on
Computational Methods in Structural Dynamics and Earthquake Engineering
M. Papadrakakis, V. Papadopoulos, V. Plevris (eds.)
Crete Island, Greece, 25–27 May 2015

DESIGN METHODOLOGY FOR SEISMIC UPGRADING OF TORSIONALLY UNBALANCED EXISTING R.C. BUILDINGS

Georgia E. Thermou[1] and Manousos Psaltakis[1]

[1]Aristotle University of Thessaloniki
Dept. of Civil Engineering, 54124, Thessaloniki, Greece
gthermou@civil.auth.gr; manousoscivil@hotmail.gr

Keywords: Assessment, Retrofitting, Torsion, Buildings, Reinforced Concrete.

Abstract.

This paper presents a design methodology for the seismic upgrading of rotationally sensitive existing R.C. buildings. The first part of the methodology deals with the elimination of the effect of torsional coupling on modal periods and shapes. The second part aims at the modification of the response shape of the building in each direction so as to achieve a near – uniform distribution of interstorey drift along the building height. A three-storey building constructed in the early 1970s with old type reinforcement detailing is selected as a case study. After being assessed, the proposed methodology is implemented and the various steps involved are described in detail. The validity of the proposed methodology was assessed by carrying out inelastic analyses with the use of a three-dimensional finite element model of the retrofitted structure. The results indicate the efficiency of the proposed design methodology for the seismic upgrading of existing torsionally unbalanced R.C. buildings.

1 INTRODUCTION

The vast majority of existing R.C. buildings stock has been designed with out-of-date codes where seismic detailing was at a primitive stage of knowledge. Recent earthquakes occurred worldwide (e.g. Northridge, California (1994); Kobe, Japan (1995); Chi Chi, Taiwan (1999); Athens, Greece (1999), Izmit and Düzce, Turkey (1999), L' Aquila, Italy (2009), Haiti (2010)) have demonstrated the susceptibility of non-ductile buildings with deficiencies related to member- and/or system-level. Insufficient reinforcement detailing of components (e.g. inadequately anchored transverse and longitudinal reinforcement, sparse and smooth stirrups, lap splices in the region of the plastic hinge, no stirrups in the beam-column joints, bad connection of the ground floor columns to the foundation system) limit the ability of the structure to resist seismic loading. System-level deficiencies such as eccentricities of stiffness and mass in both plan and elevation are common in existing structures leading to severe damage and eventually to collapse. Irregularities along the vertical axis are due to either irregular distribution of mass or stiffness along the height of the building. A special case is the soft-storey formation in pilotis type buildings (i.e. the ground storey used for commercial facilities is an open frame (bare frame), while the storeys above are infilled.). The uneven distribution of stiffness in plan (horizontal irregularities) may be the result of architectural (e.g. L-shaped buildings) or functional (e.g. facade of commercial buildings) features. The position of the elevator shaft walls plays an important role in the distribution of stiffness in plan (Fig. 1).

Figure 1: Collapse of torsionally unbalanced R.C. buildings in the 1999 Athens earthquake.

Different retrofit strategies may be developed for non-ductile R.C. buildings depending among other parameters on the mandated level of the intervention and the financial objectives of the retrofit offer [1]. Thermou et al. [2] developed a retrofit design concept according to which response may be improved by targeting for a fundamental mode shape that would produce a desirable pattern of interstorey drift and therefore damage. This concept was further extended by Pardalopoulos and Pantazopoulou [3] in three-dimensional structures with torsional component in their lateral response, where in the methodology developed the fundamental translational mode shape is approximated by separating the contributions to translation and twisting from the corresponding basic modes of an associated decoupled system.

In the proposed retrofit design methodology the criteria that need be satisfied are correction of any irregularities in plan and in elevation and elimination of mechanisms likely to lead to damage localization. Distribution rather than localization of damage is crucial; otherwise the weakest link will jeopardize the stability of the whole structure [2]. Another important issue is the modification of the structural system so as to achieve increase in the redundancy of the lateral load resisting system.

This paper presents a design methodology for the seismic upgrading of rotationally sensitive existing R.C. buildings. The methodology aims first to eliminate the effect of torsional coupling on modal periods and shapes. After this stage, the building is expected to respond independently in the two lateral directions (since torsional effects have been neglected) following the corresponding fundamental mode shapes. Next, the translational response shape in each orthogonal direction is engineered as to achieve a near – uniform distribution of interstorey drift along the building height [2]. The proposed methodology was implemented to an existing three-storey building constructed in the early 1970s. The validity of the proposed methodology was assessed by carrying out inelastic analyses with the use of a three-dimensional finite element model of the retrofitted structure. The results indicate the efficiency of the proposed design methodology for the seismic upgrading of existing torsionally unbalanced R.C. buildings.

2 FUNDAMENTALS OF THE PROPOSED RETROFIT DESIGN METHODOLOGY

The proposed retrofit design methodology aims to modify radically the response of old substandard R.C. buildings with torsional sensitivity. For this scope a retrofit design methodology has been developed which comprises two design stages (Phase I and Phase II). First, structural eccentricities are minimized and simultaneously torsional resistance and stiffness are enhanced. This is realized by the addition of stiffness at the periphery of the building through adoption of global intervention methods (e.g. R.C. infill walls, R.C. jacketing). At the end of this design stage (Phase I), the building is symmetric in plan and torsionally balanced. Thus, the ground motion in the two orthogonal axes (x and y) will cause only lateral motion, whereas the system will experience no torsional motion unless the base motion includes rotation about the vertical axis. The building is modified further as to respond in each lateral direction according to a target response shape, called hereafter target response shape. The objective is to mitigate damage localization through controlled modification of the lateral response shape. This is achieved by a weighted distribution of additional stiffness along the height of the building ([2], [4], [5]).

2.1 Elimination of the torsional sensitivity – Design Phase I

The unsymmetric plan depicted in Fig. 2(a) corresponds to the constant floor plan of an existing mulitistorey R.C. building. Due to the distance between the center of mass (CM) and the center of stiffness (CS) (i.e. eccentricities e_x and e_y in Fig. 2(a)), the building is expected to simultaneously undergo lateral motion in the two orthogonal directions (x and y) and torsion about the vertical axis whenever subjected to the x- or y-component of ground motion. In case that the origin of the xOy coordinate system is defined at the CM for each vertical member i the translational and rotational stiffness are defined as:

$$\text{Translational stiffness: } K_x = \sum_{i=1}^{n} K_{x,i} \;;\; K_y = \sum_{i=1}^{n} K_{y,i} \tag{1a}$$

$$\text{Rotational stiffness: } K_z = \sum_{i=1}^{n} \left(K_{y,i} \cdot x_i^2 + K_{x,i} \cdot y_i^2 \right) \tag{1b}$$

where $K_{x,i}$, $K_{y,i}$ are the lateral stiffness of the individual floor elements and x_i, y_i is the distance of the geometrical center of each element from the origin xOy. Note the translational and rotational stiffness as defined in Eqs. (1) correspond to the CM. The floor rotation, θ, as a result of force V_o acting at the CM is:

$$\theta = \frac{M_v}{K_z^/} = \frac{-V_o \cdot \cos a \cdot e_y + V_o \cdot \sin a \cdot e_x}{K_z^/} \tag{2}$$

where $K_z^/$ is the rotational stiffness defined at the CS according to:

$$K_z^/ = \sum_{i=1}^{n} \left[K_{y,i} \cdot \left(x_i - e_x \right)^2 + K_{x,i} \cdot \left(y_i - e_y \right)^2 \right] \tag{2a}$$

The eigenvalue problem of the existing building whose solution provides the natural frequencies, ω_s, and modes, $\mathbf{\Phi_s}$, is described mathematically by:

$$\begin{gathered}\left[\underline{\mathbf{K}} - \omega_s^2 \cdot \underline{\mathbf{M}} \right] \cdot \underline{\mathbf{\Phi}} = 0 \Rightarrow \omega_s^2 \cdot \underline{\mathbf{M}} \cdot \underline{\mathbf{\Phi}} = \underline{\mathbf{K}} \cdot \underline{\mathbf{\Phi}} \Rightarrow \\ \omega_s^2 \cdot \begin{bmatrix} \mathbf{m} & \mathbf{0} & \mathbf{0} \\ \mathbf{0} & \mathbf{m} & \mathbf{0} \\ \mathbf{0} & \mathbf{0} & \mathbf{J_m} \end{bmatrix} \cdot \begin{Bmatrix} \mathbf{\Phi_x} \\ \mathbf{\Phi_y} \\ \mathbf{\Phi_z} \end{Bmatrix} = \begin{bmatrix} \mathbf{K_x} & \mathbf{0} & \text{-}e_y \cdot \mathbf{K_x} \\ \mathbf{0} & \mathbf{K_y} & e_x \cdot \mathbf{K_y} \\ \text{-}e_y \cdot \mathbf{K_x} & e_x \cdot \mathbf{K_y} & \mathbf{K_z} \end{bmatrix} \cdot \begin{Bmatrix} \mathbf{\Phi_x} \\ \mathbf{\Phi_y} \\ \mathbf{\Phi_z} \end{Bmatrix}\end{gathered} \tag{3}$$

where ω_s (s=x,y,z) is the natural frequency, $\mathbf{K_x}$, $\mathbf{K_y}$, $\mathbf{K_z}$ are the diagonal submatrices of the translational stiffness in x and y direction and of the rotational stiffness of order N/3 (N is the number of storeys). $\mathbf{\Phi_s}^T=[\Phi_{s,1}, \Phi_{s,2},\ldots, \Phi_{s,N}]^T$ (s=x, y, z) are the mode shapes of the system. $\mathbf{m}$, $\mathbf{J_m}$ are the diagonal submatrices of the mass and moment of inertia of order N/3 (N is the number of storeys). The moment of inertia at each storey is defined as:

$$J_m = m_{st} \frac{\left(L_x^2 + L_y^2 \right)}{12} = m_{st} \cdot l_s^2 \tag{4}$$

where m_{st} is the storey mass, L_x, L_y are the in plan dimensions of the building and l_s is the radius of gyration of the floor mass in plan.

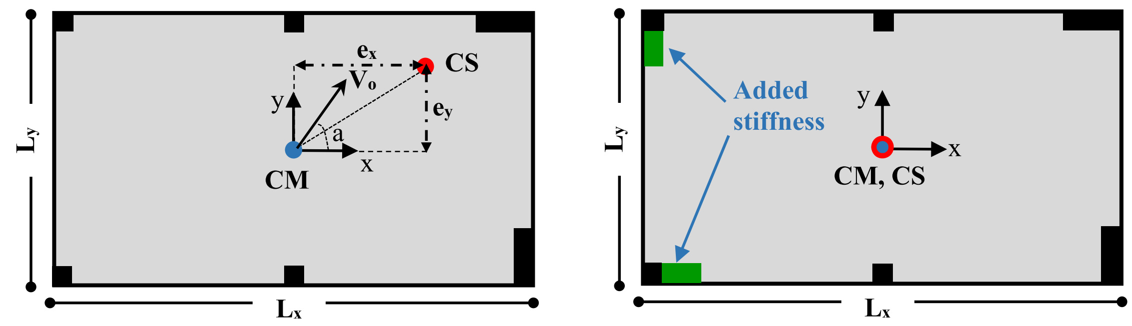

Figure 2: Plan layout (a) of the existing building; (b) of the retrofitted building (eccentricity elimination).

The mode shapes are coupled through the stiffness matrix, **K**, because the stiffness properties are not symmetric about the x and y axes. In case that eccentricity could be eliminated so that $\mathbf{K_{x\theta}}=\mathbf{K_{\theta x}}=\mathbf{K_{y\theta}}=\mathbf{K_{\theta y}}=0$ (i.e. $e_x=e_y=0$ and thus $\theta=0$ (Eq. (2)), then the system would be uncoupled in x, y and z directions. This can be achieved by adding stiffness to the system in strategically selected positions at the periphery of the building as to minimize eccentricity and simultaneously increase torsional resistance (Fig. 2(b)). The translational and rotational stiffness of the modified system are:

$$\text{Translational stiffness: } K_x^R=\sum_{i=1}^{n}K_{x,i}+\sum_{p=1}^{m}K_{x,p}\ ;\ K_y^R=\sum_{i=1}^{n}K_{y,i}+\sum_{q=1}^{\ell}K_{y,q} \tag{5a}$$

$$\text{Rotational stiffness: } K_z^R=\sum_{i=1}^{n}\left(K_{y,i}\cdot x_i^2+K_{x,i}\cdot y_i^2\right)+0.25\cdot L_x^2\cdot\sum_{q=1}^{\ell}K_{y,q}^R+0.25\cdot L_y^2\cdot\sum_{p=1}^{m}K_{x,p}^R \tag{5b}$$

where $\sum_{p=1}^{m}K_{x,p}$ and $\sum_{q=1}^{\ell}K_{y,q}$ refer to the additional stiffness required as to remove any eccentricity of the floor plan. The objective is to add such an amount of stiffness as to move the CS to the CM (i.e. $e_x=e_y=0$ in Fig. 2(a)). Hence, the required amount of stiffness in the x direction may be estimated from:

$$x_{CM}=x_{CS}=0\Rightarrow\frac{\sum_{i=1}^{n}\left(K_{x,i}\cdot y_i\right)+0.5\cdot L_y\cdot\sum_{p=1}^{m}K_{x,p}}{\sum_{i=1}^{n}K_{x,i}+\sum_{p=1}^{m}K_{x,p}}=0\Rightarrow\sum_{p=1}^{m}K_{x,p}=-\frac{2}{L_y}\sum_{i=1}^{n}\left(K_{x,i}\cdot y_i\right) \tag{6a}$$

Similarly, the required amount of stiffness in the y direction is:

$$\sum_{q=1}^{\ell}K_{y,p}=-\frac{2}{L_x}\sum_{i=1}^{n}\left(K_{y,i}\cdot x_i\right) \tag{6b}$$

Eq.(3) that describes the eigenvalue problem for the existing building is modified accordingly as to account for the effect of the additional stiffness that lead to elimination of eccentricity and enhancement of the torsional resistance:

$$\omega_s^2 \cdot \begin{bmatrix} \mathbf{m} & \mathbf{0} & \mathbf{0} \\ \mathbf{0} & \mathbf{m} & \mathbf{0} \\ \mathbf{0} & \mathbf{0} & \mathbf{J_m} \end{bmatrix} \cdot \begin{Bmatrix} \mathbf{\Phi_x^R} \\ \mathbf{\Phi_y^R} \\ \mathbf{\Phi_z^R} \end{Bmatrix} = \begin{bmatrix} \mathbf{K}_x^R & \mathbf{0} & \mathbf{0} \\ \mathbf{0} & \mathbf{K}_y^R & \mathbf{0} \\ \mathbf{0} & \mathbf{0} & \mathbf{K}_z^R \end{bmatrix} \cdot \begin{Bmatrix} \mathbf{\Phi_x^R} \\ \mathbf{\Phi_y^R} \\ \mathbf{\Phi_z^R} \end{Bmatrix} \tag{7}$$

Thus, the three uncoupled equations that describe the eigenvalue problem are:

$$\omega_x^2 \cdot \mathbf{m} \cdot \mathbf{\Phi_x^R} = \mathbf{K}_{\mathbf{x}}^{\mathbf{R}} \cdot \mathbf{\Phi_x^R}\,;\omega_y^2 \cdot \mathbf{m} \cdot \mathbf{\Phi_y^R} = \mathbf{K}_{\mathbf{y}}^{\mathbf{R}} \cdot \mathbf{\Phi_y^R}\,;\ \omega_z^2 \cdot \mathbf{m} \cdot \mathbf{\Phi_z^R} = \mathbf{K}_{\mathbf{z}}^{\mathbf{R}} \cdot \mathbf{\Phi_z^R} \tag{8}$$

According to Eq. (8) the modified building (Fig. 2(b)) will response independently in the two lateral directions (torsional effects have been neglected) following the corresponding fundamental mode shapes.

2.2 Strengthening for a target response shape – Design Phase II

In the proposed rehabilitation framework, deformation demand is quantified by interstory drift throughout the structure. In a reverse process of redesign, in which the desirable pattern of interstorey drift distribution prescribes the proper morphology of the fundamental mode shape, it is relatively straightforward to evaluate the pattern of stiffness distribution throughout the structure that is required to produce a desirable translational mode ([5], [6], [7]). The retrofit design methodology developed by Thermou et al. [6] is adopted. In the first step of the methodology the target period of the retrofitted building, T_{target}, is defined. It could range between $0.05H_{tot}^{3/4} \leq T_{target} < T_{existing}$. The Yield Point Spectrum (YPS) representation [8] is utilized for defining for a given period value, T_{target}, the total acceleration and relative displacement coordinates of the elastic ADRS spectrum (corresponding to T_{target}) which are simply divided by the behaviour factor, q_{target}, and the corresponding ductility demand, μ_{target}. A ductility value (μ_{target}) between 2 and 3 may be considered achievable for retrofitted buildings. Next, the target response shape, Φ_{shape}, is selected. The driving consideration is the pursuit to obtain as nearly uniform as possible a distribution of drift demand. Alternative options for the selected response shape are presented in Fig. 3. When considering structural vibration in the selected target mode shape, the generalized (effective) SDOF properties of the structure are related to the target period and from there to the required secant-to-yield stiffness of the first floor, K_1, as follows:

$$T_{target} = 2\pi\sqrt{\frac{M^*}{K^*}} = 2\pi\sqrt{\frac{m \cdot w_1}{K_1} \cdot \frac{\sum_{j=1}^{N} \Phi_j^2}{\sum_{j=1}^{N} w_j \cdot \Delta\Phi_j^2}} \Rightarrow K_1 = \frac{4\pi^2}{\left(T_{target}\right)^2}\left(m \cdot w_1 \frac{\sum_{j=1}^{n} \Phi_j^2}{\sum_{j=1}^{n} w_i \cdot \Delta\Phi_j^2}\right) \tag{9a}$$

where K_1 is the stiffness of the first storey, w_1 is the weighting factor value at the first storey, m is the typical storey mass, Φ_j is shape value at the jth storey (N is the total number of storeys) and T_{target} is the target period. Eq. (9a) may be further simplified in case of a triangular response shape with equal storey height to:

$$K_1 = \frac{4\pi^2}{\left(T_{target}\right)^2}\left(m \cdot w_1 \cdot \sum_{j=1}^{N} i\right) \tag{9b}$$

The required stiffness in the *j*-th floor associated with the selected target shape is obtained from:

$$K_j = \frac{w_j}{w_1} K_1 \tag{10}$$

This procedure is repeated in both lateral directions. The additional stiffness required at each storey in both lateral directions as for the lateral response shape to conform to the target shape is distributed along the vertical members of the floor. In the selection of the vertical members to be strengthened attention should be paid as not to modify the center of stiffness.

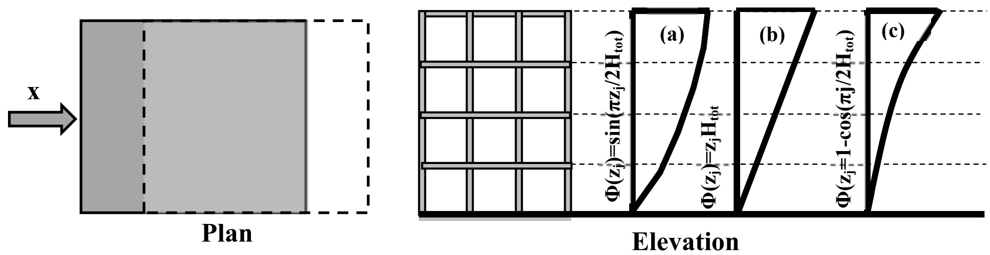

Figure 3: Lateral displacement profiles; (a) shear; (b) triangular; (c) flexural.

3 IMPLEMENTATION OF THE PROPOSED RETROFIT DESIGN METHODOLOGY

3.1 Description of the Existing Building

The building selected as a case study is a 3-storey residential R.C. building constructed in the center of the city of Thessaloniki (North Greece) in the early 1970s according to the provisions of the first Greek Seismic Code [9]. The first storey (ground floor) has a commercial use (windows at the perimeter - open first storey) whereas the other floors are used as apartments. The plan layout of the first storey is differentiated. The first storey height is 4.50 m whereas the height of the other two floors is 3 m. The area of the typical floor is 351.68m^2 and is constant along the height of the building.

The structural system is formed as an orthogonal grid of columns, walls, beams and slabs (Fig. 4). As it is observed there are a few beam to beam connections. Discontinued (cut-off) columns do not exist.

The cross section of the columns is rectangular with varied dimensions along the building's height, generally reducing by 5 cm in each upper floor. The average column in the ground floor is 35cm square and is reduced up to 25cm square in the last floor. Columns longitudinal reinforcement comprises smooth bars of 12 mm ÷ 20 mm diameter and the longitudinal reinforcement over the column section ranged between 6.6‰ ÷ 10.3‰. Column transverse reinforcement comprises stirrups of 6 mm bar diameter spaced at 250 mm anchored with 90° hooks in the ends. The influence of the shear reinforcement is considered negligible, due to the small diameter and the sparse placement of the transverse reinforcement.

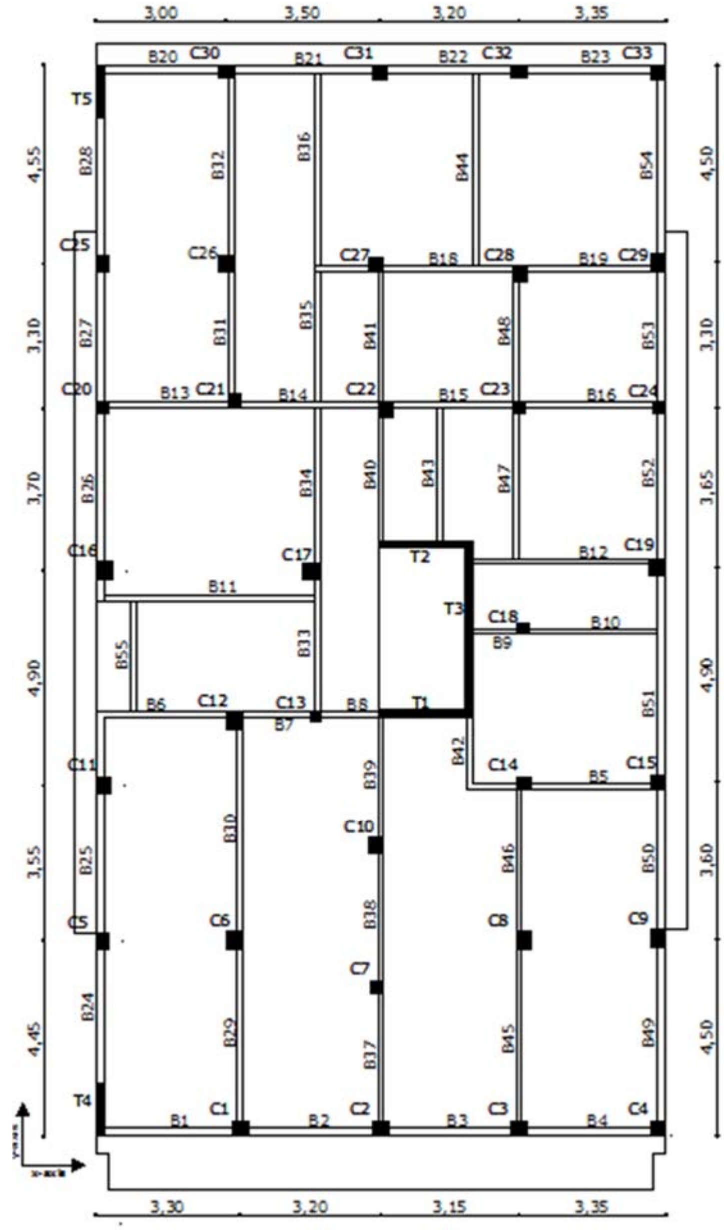

Figure 4: Typical plan layout of the 1st storey.

The geometry and the reinforcement detailing of R.C. walls followed the typical construction practice of that era in Southern Europe. The dimensions of the wall cross section were 1200 mm ÷ 2150 mm long by 150 mm ÷ 250 mm in width. The boundary elements were lightly reinforced by 4∅12 mm longitudinal bars and the web reinforcement comprised of a dual mesh ∅8/250 mm.

The longitudinal reinforcement of the beams comprises smooth bars of varying diameter 10 mm ÷ 20mm and longitudinal reinforcement area ratio tanged between 3.1‰ ÷ 14.7‰ approximately. Note that in a few beams three different bar diameters are placed (e.g. 10 mm, 12 mm and 16 mm). Transverse reinforcement follows the same pattern as in columns. The slab thickness was 0.10 m constant at all floors and considered to offer diaphragmatic action.

The materials considered were B160 concrete quality (which corresponds to f_{ck}=10 MPa) and smooth StI for longitudinal and transverse reinforcement of the structural members (f_{sy}=f_{syw}=250 MPa).

Gravity load was estimated by considering the load combination g+0.3q (dead load and 30% of the live load). Finishing were taken 0.6 kN/m^2 and live load 2 kN/m^2 according to the information found in the folder of the project. The balcony load was applied as uniform load on the external beams providing an additional dead load of 3.40 kN/m and live load of 5.00 kN/m.

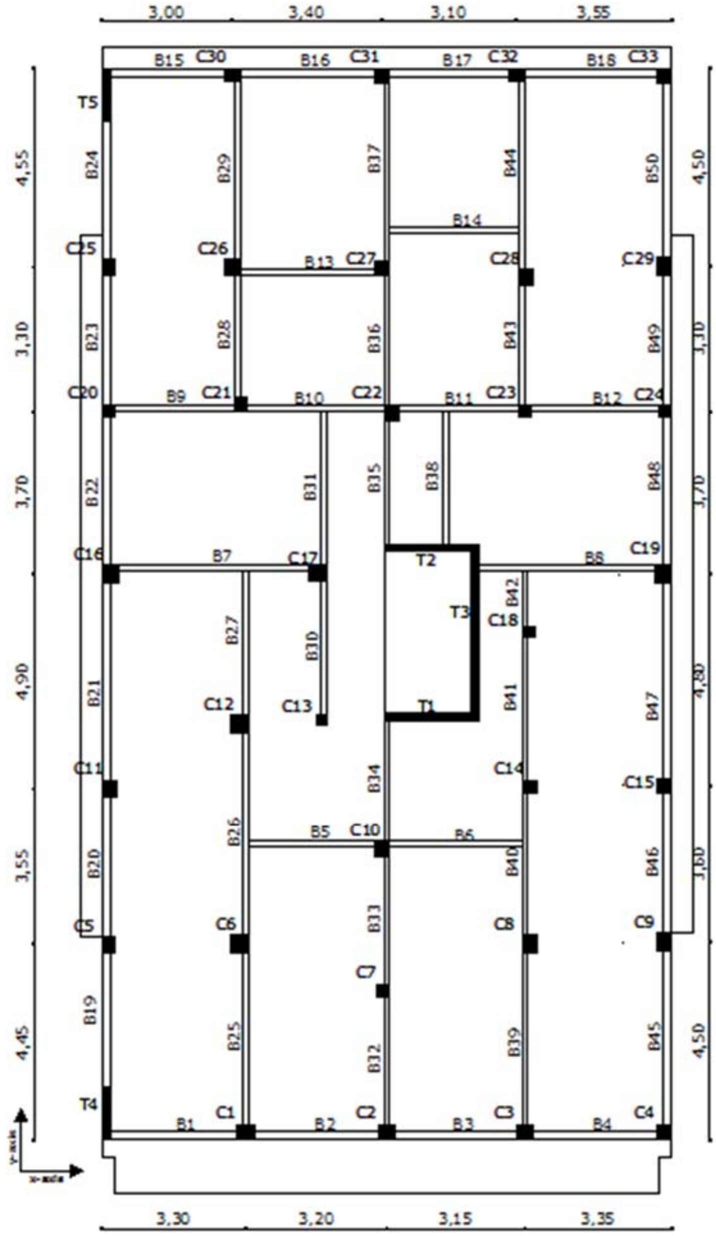

Figure 5: Typical floor plan layout of the 2nd and 3rd storey.

3.2 Assessment of the Existing Building

Before proceeding with the implementation of the proposed retrofit design methodology, a pre-requisite step is the assessment of the existing building. Structural regularity is checked first and then assessment at member level is performed as to define the deformation and strength capacity of all the structural members. Moreover, assessment through detailed analysis was also performed as to verify the results of the hand calculations.

3.2.1 Check of Regularity in Plan and Elevation

The EC8-Part I [10] quantified criteria for assessing structural regularity are implemented. The slenderness, $\lambda(=L_{max}/L_{min})$, of the case study building is 1,90 (λ=1,90<4), thus less than 4,0. The structural eccentricity in both directions x-x and y-y, $e_{o,x}$ and $e_{o,y}$, is smaller than 30% of the torsional radius in both horizontal directions (Table 1). The torsional radius, r_x and r_y, is larger than the radius of gyration in direction x and smaller in direction y. As a result, the building is characterized as being irregular in plan only in the x-x direction.

Table 1: Check of regularity in plan

Direction x-x						**Direction y-y**					
e_{ox}<	0,30 r_x	Check	r_x>	l_s	Check	e_{oy}<	0,30 r_y	Check	r_y>	l_s	Check
1,09<	1,61	√	5,36	7,99	X	0,02	2,53	√	8,43	7,99	√
Conclusion: Irregularity in plan						**Conclusion: Regularity in plan**					

The building evidently fulfills all requirements for regularity in elevation stated in EN 1998-Part I [10]. Specifically, all lateral load resisting systems run without interruption from the foundation to the top of the building. The lateral stiffness and the mass of the individual storeys remain constant from the base to the top of the building.

3.2.2 Assessment at Member Level

The chord rotation at yield and at ultimate, as well as the flexural and shear strength of the existing jth R.C. members (columns, beams, walls) were estimated according to EC8-Part III [11] and the Greek Intervention Code [12]. The following expressions were used:

For beams or rectangular columns:

$$\theta_{y,j} = (1/r)_y \frac{L_S+a_v z}{3} + 0{,}0014\left(1+1{,}5\frac{h}{L_S}\right) + \frac{(1/r)_y d_b f_y}{8\sqrt{f_c}} \tag{11a}$$

For walls:

$$\theta_{y,j} = (1/r)_y \frac{L_S+a_v z}{3} + 0{,}0013 + \frac{(1/r)_y d_b f_y}{8\sqrt{f_c}} \tag{11b}$$

For beams or rectangular columns:

$$\theta_{um,j} = 0{,}016(0{,}3^{\nu})\left[\frac{\max(0{,}01;\omega')}{\max(0{,}01;\omega)}f_c\right]^{0.225}(a_s)^{0{,}35}25^{\left(a\rho_s\frac{f_{sw}}{f_c}\right)}(1{,}25^{100\rho_d}) \tag{11c}$$

, where a_v=1 if the shear force at flexural yielding, M_y/L_s, exceeds the shear at diagonal cracking, or 0 otherwise, z is internal lever arm equal to 0.9d in beams or columns, $0.8l_w$ in walls, d_b: diameter of longitudinal bars, a_w=1 for walls, 0 otherwise; ρ_s: confining reinforcement ratio in the direction of bending; ρ_d is diagonal reinforcement ratio. Material strengths f_y, f_c are in MPa. In members not detailed for earthquake resistance, the right hand of Eq (11c) is reduced by 20%. For every vertical member the flexural strength, V_y, was estimated by considering EC8-III [11] and KANEPE [12] expressions according to which flexural capacities are converted into associated shear forces, $V_y=M_y/Ls$. This may be done assuming attainment of flexural capacity at both ends for the columns (shear span L_s equal to half the clear storey height), or a shear span L_s of walls equal to 2/3 of the total height of the building. The yield moment, M_y, may be computed according to Eq (12).

$$\frac{M_{y,j}}{bd^3} = (1/r)_{y,j} \left\{ \begin{matrix} E_C \frac{{\xi_{y,j}}^2}{2}\left(0.5(1+\delta') - \frac{\xi_{y,j}}{3}\right) + \left[(1-\xi_{y,j})\rho + (\xi_{y,j} - \delta')\rho' + \frac{\rho_v}{6}(1-\delta')\right] \\ (1-\delta' \frac{E_S}{2} \end{matrix} \right\} \tag{12}$$

According to KANEPE [12] the secand-to-yield at each end of a concrete member, EI_{eff}, may be computed from the yield moment, M_y, and the chord rotation at yielding at the end, θ_y, as:

$$EI_{eff,j} = M_{y,j}L_s/3\theta_{y,j} \tag{13}$$

In this study, it is assumed that the columns of the storey are fixed in both ends whereas walls are fixed only at the base. Thus, the shear span for the columns is equal to half the clear storey height whereas for the walls it was taken equal to 2/3 of the total height of the building (i.e. they are considered to behave as cantilevers with a height equal to $2/3H_{tot}$). Thus, the stiffness, K_j, of the i[th] vertical member is:

For columns:
$$K_j = M_{y,j}/\left(2 \cdot \theta_{y,j} \cdot {L_S}^2\right) \tag{14a}$$

For walls:
$$K_j = M_{y,j}/\left(\theta_{y,j} \cdot {L_S}^2\right) \tag{14b}$$

From the above, the stiffness at member level is estimated. The total stiffness of each floor is obtained by direct summation of the stiffness of the individual vertical members of each floor (they are considered to function as a sequence of springs in parallel) and presented in Tables 2:

Table 2: Stiffness of the building for each storey and at each direction

Stiffness, K_j (kN/m)		
Storey	direction x	direction y
1st	87077,12	96447,9
2nd	165381,76	181295,15
3rd	127008,98	137747,31

The shear resistance of beams, columns and walls, $V_{R,i}$, with rectangular web (with units: MN and meters) was calculated according to:

$$V_{R,i}=\frac{h-x}{2L_s}\min\left(N;0{,}55A_{c,i}f_c\right)+\left(1-0{,}05\min\left(5,\mu_{\theta,i}^{pl}\right)\right)\left[0{,}16\max\left(0{,}5;100\rho_{tot,i}\right)\left(1-0{,}16\min(5;a_s)\right)\sqrt{f_c}A_{c,i}+V_{w,i}\right] \quad (15)$$

The shear strength of a concrete wall, $V_{R,i}$, may not be taken greater than the value corresponding to failure by web crushing, $V_{R,max,i}$, which under cyclic loading may be calculated from the following expression (with units: MN and meters):

$$V_{R,max,i}=0{,}85\left(1-0{,}06\min\left(5;\mu_{\theta,i}^{pl}\right)\right)\left(1+1{,}8\min\left(0{,}15;\frac{N_i}{A_{c,i}f_c}\right)\right)\left(1+0{,}25\max\left(1{,}75;100\rho_{tot,i}\right)\right)\left(1-0{,}2\min(2;a_s)\right)\sqrt{f_c}b_{w,i}z_i \quad (16)$$

where $\mu_{\theta,i}^{pl}$ is the ratio the plastic part of the chord rotation, θ, normalized to the chord rotation at yielding, θ_y. In the calculations, $\mu_{\theta,i}^{pl}$ was assumed equal to 0. The results of the shear strength assessment of the columns and the walls are presented in Table 3. As it is shown in case of columns premature failure in shear is expected to occur in all the floors. This corresponds to the case that index v (=$V_{shear,c}/V_y$) < 1 (Table 3). This implies that the columns will fail well before reaching yielding and thus the chord rotation at yielding will not be reached. Instead the columns at the time of failure will have a chord rotation significantly reduced (almost half) of the chord rotation at yielding (Table 3). The value of 0.25% can be considered representative for all the floors. Referring to the walls no premature failure is anticipated.

Table 3: Average values of chord rotation at yielding and ultimate and shear resistance of the vertical members

Floor		$\theta_{y,col}^{flex*}$ (%)	$\theta_{u,col}^{flex*}$ (%)	$V_{shear,c}$ (kN)	V_y (kN)	$v=V_{shear,c}/V_y$	Failure	$\theta_{fail}^{*}= v\cdot\theta_{y,col}^{flex}$ (%)
1st	Columns (C1-C33)	0,44	0,61	22,26	38,21	0.58	Shear	0.26
2nd		0,41	0,56	29,75	46,19	0.64	Shear	0.26
3rd		0,41	0,55	21,00	34,79	0.60	Shear	0.25
		$\theta_{y,wall}$ (%)	$\theta_{u,wall}$ (%)	$V_{shear,w}$ (kN)	V_y (kN)	$v=V_{shear,c}/V_y$	Failure	$\theta_{fail}^{*}= v\cdot\theta_{y,col}^{flex}$ (%)
Walls	direction x-x (T1-T2)	0,34	3,19	691,20	127,59	5.42	Flexure	-
	direction y-y (T3-T5)	0,43	3,45	691,20	127,59	5.42	Flexure	-

* The same value applies in both directions x-x, y-y due to the square cross section

3.2.3 Assessment through Detailed Analysis

The finite element analysis program SeismoStruct v6.5 is utilized to perform necessary analysis for the assessment of existing building such as nonlinear static pushover analysis, eigenvalue analysis and incremental dynamic analysis. Both vertical and horizontal elements are modeled with inelastic elements capable of representing progressive cracking and spread of inelasticity. Beam-column joints are assumed rigid and fully-fixed boundary conditions are adopted at the base of the building (Fig. 6).

Figure 6: 3D modeling of the existing R.C. building

3.2.3.1. Eigenvalue Analysis

Eigenvalue analysis was performed for determining the periods and mode shapes as presented in Table 4 and Fig. 7. The torsional sensitivity of the building due to the irregularity in plan in x-x direction is verified by the eigenvalue analysis.

Table 4: Elastic periods and modal participation mass ratios of the existing building

Mode shape No.	Period (s)	Modal participation mass ratio		
		Ux	Uy	Rz
1	0,683	0,22%	4,55%	90,43%
2	0,634	84,15%	0,07%	0,13%
3	0,373	0,04%	80,92%	4,53%

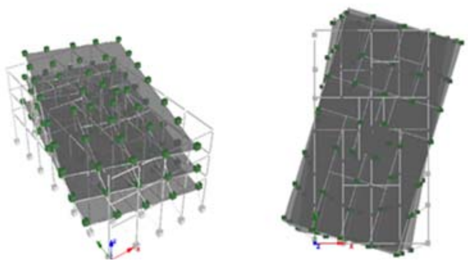

(a) 1st mode: T_1=0.68s MPMR=90.43%

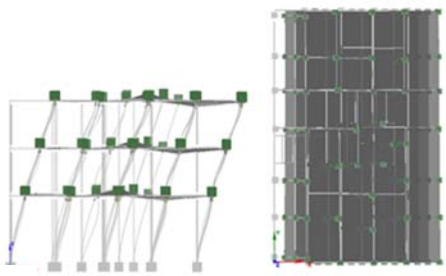

(b) 2nd mode: T_2=0.63s MPMR=84.15%

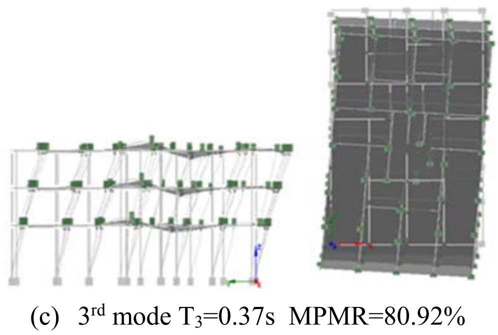

(c) 3rd mode T_3=0.37s MPMR=80.92%

Figure 7: Deformed shape, periods and modal participating mass ratio (MPMR) of the existing building: (a) 1st mode; (b) 2nd mode; (c) 3rd mode

3.2.3.2 Pushover Analysis

In case of torsionally sensitive buildings static pushover analysis exhibits shortcomings and limitations that confine its range of application and raise doubts of its effectiveness to accurately estimate structural seismic demand, as demonstrated by a number of researchers [e.g. [13], [14]). However, according to the Greek Code for interventions [11], pushover analysis is permitted to be implemented even in torsionally unbalanced buildings, only when accompanied by a non-linear dynamic analysis for validation reasons. Thus, incremental dynamic analyses are performed for various ground motions in order to assess the level of validity of the pushover analyses results. Incremental dynamic analyses (IDA) are performed only for the direction where the structure is torsionally unbalanced (direction y-y). Eurocode 8-III [11] requires the use of a spatial model in case of building not conforming with the criteria for regularity in plan.

The building was subjected to pushover analyses separately in the two orthogonal directions x-x and y-y. Two different lateral force profiles were adopted, the modal and the uniform shape. From the pushover analyses conducted, it was shown that uniform distribution led always to more unfavorable results as expected. For this purpose, the results from the uniform load profile are presented. The base shear – roof displacement curve of the structure in the x-x and y-y direction is depicted in Fig. 8(a) and 8(b), respectively. The horizontal dashed line indicates the base shear force level at which shear failure is anticipated according to the assessment conducted at member level (Table 2). Hence, from the assessment failure is expected prior to global yielding.

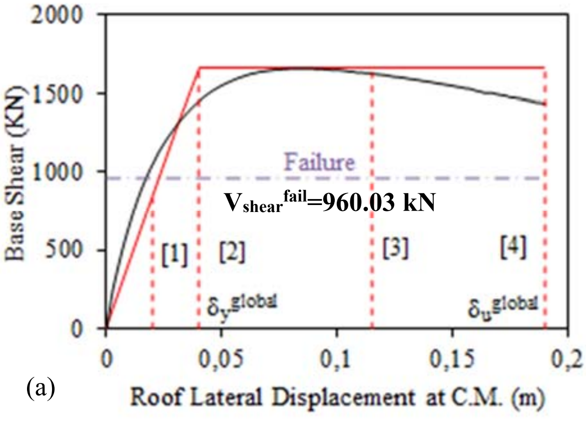

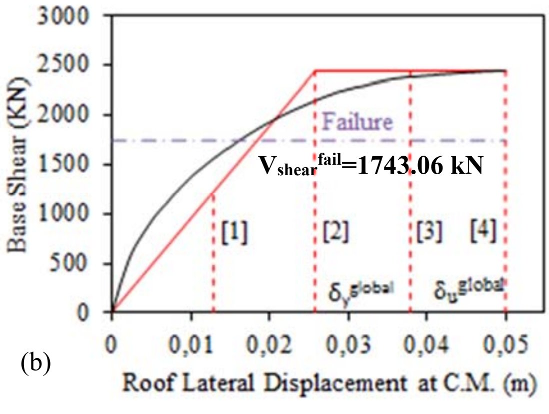

Figure 8: Pushover curves of the existing R.C. building along (a) x-x axis and (b) y-y axis

After bi-linearization of the pushover curve yielding, δ_y^{global}, and ultimate, δ_u^{global}, at global level are defined as shown in Fig. 8. The interstorey drift profile was estimated for four different deformation stages depicted as [1], [2], [3] and [4] (Fig. 8). Stage [2] and Stage [4] correspond to global yielding and ultimate, respectively, whereas Stage [1] corresponds to half the global yielding and Stage [3] to (δ_y^{global}+1/2δ_{pl}^{global}). Failure is expected when the interstorey drift level reaches a value equal to 0.25% (Fig. 9, see also Table 2). Damage is localized in the columns of the ground floor. For instance, in direction x-x 85% of the columns in 1st storey fails due to the lack of shear resistance, the same happens in the 2nd and 3rd storey with 48% and 55% of the columns to fail. Consequently, localization of damage in the first storey leads to soft storey mechanism and brittle failure mode.

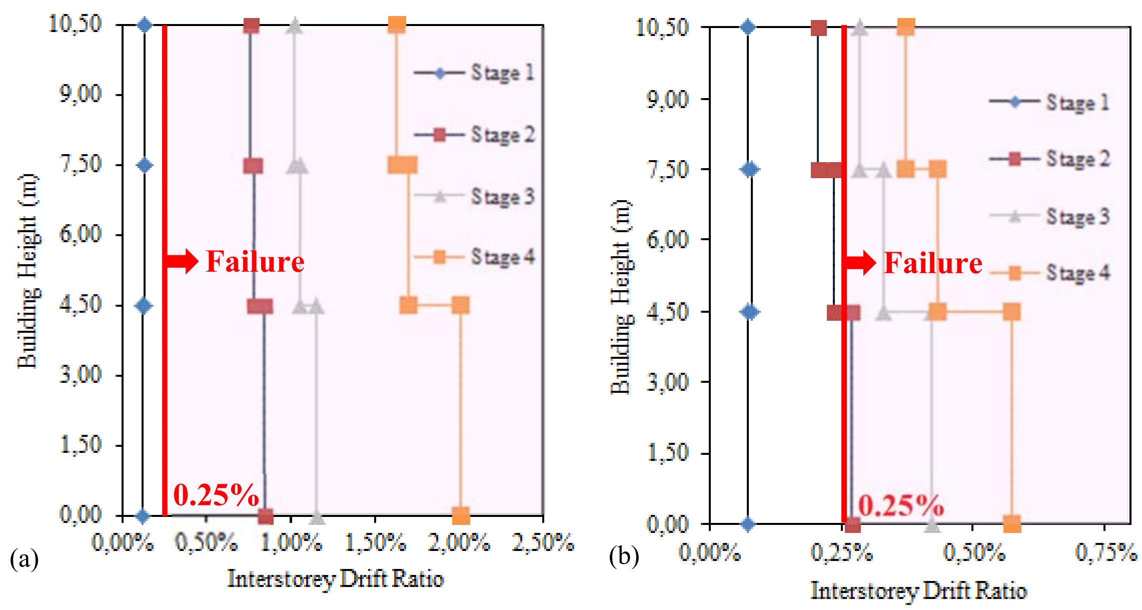

Figure 9: Interstorey drift ratio (a) along x-x axis (b) y-y axis

3.2.4.3 Response to Earthquake Excitation

Incremental dynamic analyses were performed for three different ground motions (El Centro 1940, Northridge 1994 and Loma Prieta 1989). The duration of the records is 40 seconds and the peak ground acceleration is 0.31g, 0.60g and 0.50g, for the El Centro 1940, Northridge 1994 and Loma Prieta 1989 ground motion, respectively. IDA involved performing a series of non-linear dynamic analyses for each record by scaling it to multiple levels of intensity. Five scaling factors (0.1, 0.4, 0.7 and 1.0) are selected in order to represent the seismic intensity at each time of history analysis. The comparison between static pushover curves and IDA curves is depicted in Fig. 10 and it is shown that the behavior of structure along direction y –y under static push-over analysis is similar to the behavior under dynamic analysis. The maximum base shear for the selected ground motion El Centro is 1733.0 kN, Loma Prieta is 2583.0 kN and for the Northridge is 2500.0 kN. The comparison between the pushover and the IDA curves verifies that static pushover analyses can be used for assessment.

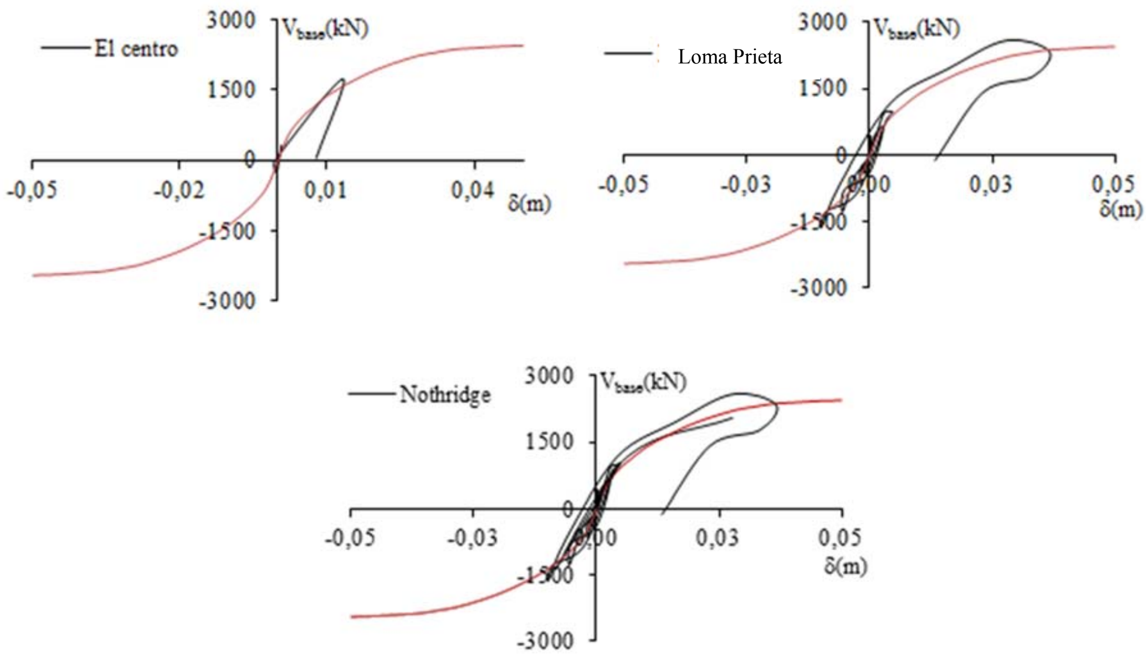

Figure 10: Comparison between static pushover and IDA analysis

3.3 Design of the Retrofit Solution

3.3.1 Elimination of the Torsional Sensitivity

The building according to the regularity in plan check is rotationally sensitive (Table 1). The first phase of the proposed retrofit design methodology involves addition of stiffness in a strategic way at the periphery of the building as to minimize structural eccentricities and increase torsional resistance. Intervention methods that may serve this scope are R.C. jacketing and the addition of R.C. walls. Table 5 indicates the required additional floor stiffness in the x-x and y-y direction for the elimination of the effect of torsional coupling on modal periods and shapes. The most efficient solution is depicted in Fig. 11. Four infill R.C. walls are added at the perimeter of the first storey, two in each direction (T9 and T10 in x-x direction, and T6 and T7 in y-y direction) and one column is jacketed C19 (Fig. 11(a)). The added R.C. walls continue to the second and third floor (Fig. 11(b)). Tables 6 and 7 present reinforcement details of the additional concrete walls and the jacketed members. The material properties of the new added members are concrete compressive strength f_{ck}=30 MPa, and nominal yield strength f_{syk}=500 MPa.

Table 5: Required stiffness for elimination of plan eccentricity

Required stiffness for (e_x=0 και e_y=0)			
	1st Floor	2nd Floor	3rd Floor
direction x-x, K_x (kN/m)	113164,88	108337,22	101868,10
direction y-y, K_y (kN/m)	120650,11	115822,20	109353,08

Table 6: Reinforcement details of the added R.C. walls

R.C. Walls									
	b_x (m)	b_y (m)	Long. Reinforcement (mm)	Stirrups (mm)	h_{fi} (m)	ρ_{itot} (%)	A_{fi} (mm)	K_x (kN/m)	K_y (kN/m)
T6	0,20	3,20	#Ø10/250	Ø10/150	0,35	1,02%	4Ø22	0	66320,0
T7	0,20	3,20	#Ø10/250	Ø10/250	0,35	0,64%	4Ø20	0	43033,1
T9	2,80	0,20	#Ø10/250	Ø10/200	0,35	0,74%	4Ø20	35577,5	0
T10	2,80	0,20	#Ø10/250	Ø10/250	0,35	0,68%	4Ø22	32053,6	0

Table 7: Reinforcement details of the R.C. jacketed members

R.C. Jacketed Columns								
		b_x (m)	b_y (m)	Long. Reinforcement (mm)	Stirrups (mm)	ρ_{itot} (%)	ΔKx (kN/m)	ΔKy (kN/m)
1st	C19	0,55	0,55	8Ø22	Ø16/100	1,01%	4407,0	4407,0
2nd	C19	R.C. jacketing of column C19 in the first floor						
3rd	C19							

3.3.2 Strengthening for a Target Interstorey Drift

Once the torsional effects of the building have been eliminated in the first phase of the methodology, the second phase deals with system-level deficiencies associated with irregular distribution of stiffness along the height of the building. The method assumes that the building responds in a single mode in each direction since twisting rotation along the vertical axis is insignificant. The retrofit scenario adopted aims to reduce the period of the existing building to a period that can range between $0{,}05H_{tot}^{3/4}=0{,}05\cdot 10{,}5^{\wedge(3/4)}=0{,}29s\leq T_{target}<T_{existing}=0{,}66s$ (average value of the period of the first and the second modes: 1/2(0,68+0,63)=0,66s, see Fig. 7). The target period was selected to be equal to half the period of the existing building T_{target}=0,33s. Ductility was assumed equal to 2 which is considered a realistic scenario for a substandard building. The triangular response shape which corresponds to equal distribution of damage along the height of the building was utilized ($\Phi^T=[0{,}43\ ,\ 0{,}71,\ 1{,}00]^T$). The target stiffness of each floor is determined through the use of the weighting factors following the procedure described in Section 2, §2.2.

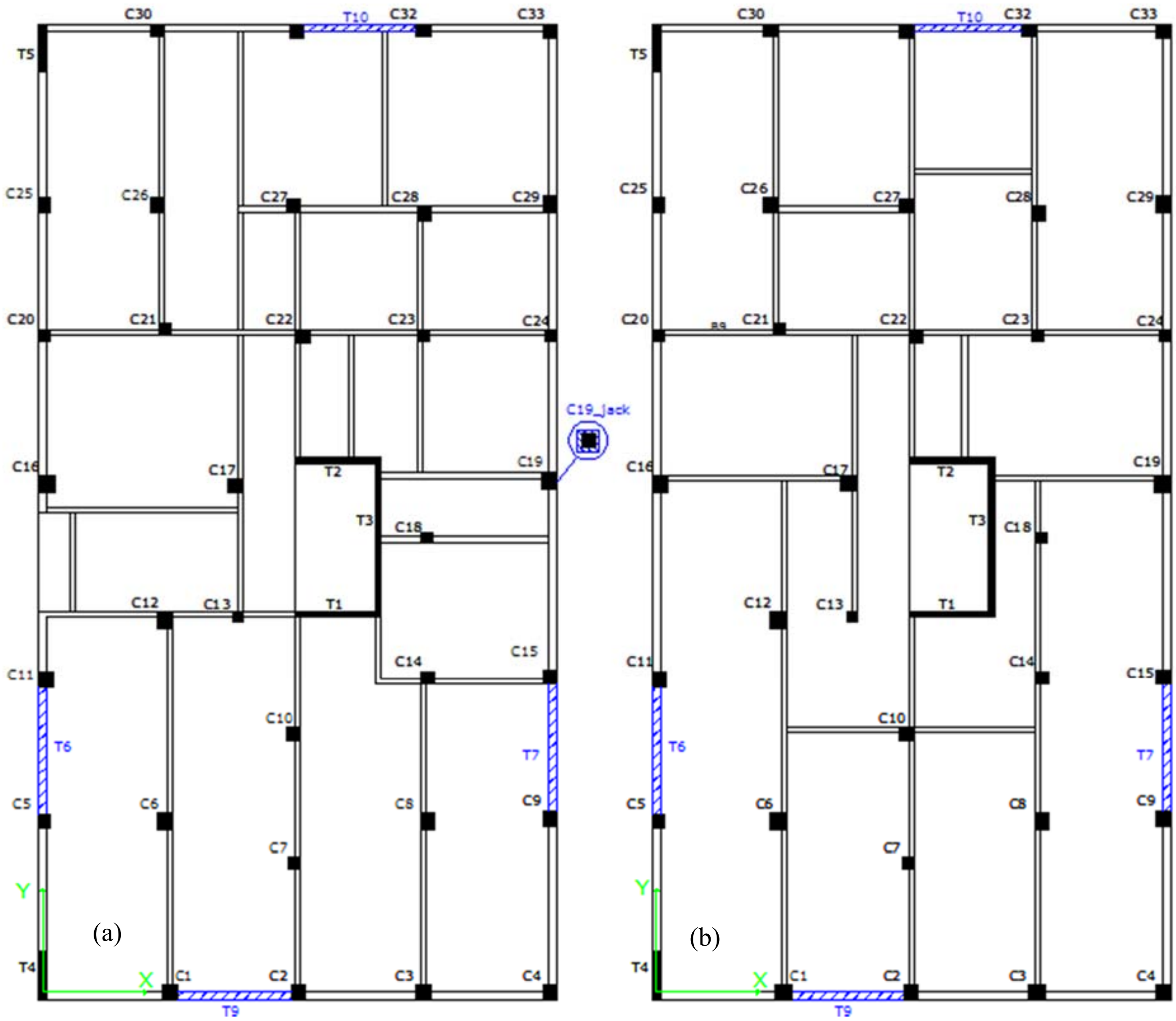

Figure 11: Addition of R.C. walls and R.C. jacketing for the elimination of torsional sensitivity (a) floor plan of first storey (b) floor plan of second and third floor

The MDOF system with storey mass m=136,25t is transformed to ESDOF system with the following characteristics:

$$M^* = \sum_{j=1}^{N} m_j \cdot \phi_j^2 = 230,79t\,;\; L^* = \sum_{j=1}^{N} m_j \cdot \phi_j = 291,96t\,;\; \Gamma = \frac{L^*}{M^*} = 1,27 \tag{17}$$

The Yield Point Spectra (YPS) of Fig. 12 were extracted from the 5% damped elastic spectrum of EC8 (2004) using the equal displacement rule (q=μ) for peak ground acceleration a_g=0.36g, soil class B, S=1.2, with corner point periods defining the various spectrum regions equal to T_B=0.15 s, T_C=0.40s and T_D=2.00s. Given the target period T_{target}=0.33s, the target displacement at yield of the ESDOF, $\delta^*_{y,\,target}$, is estimated through the YPS depicted in Fig. 12 is 14.61mm. Thus, the target drift of the MDOF system is:

$$\theta_{y,target} = \frac{\delta_{y,target}}{H_{tot}} = \frac{\delta^*_{y,target} \cdot \Gamma}{H_{tot}} = \frac{18,55}{10500} = 0.18\% \tag{18}$$

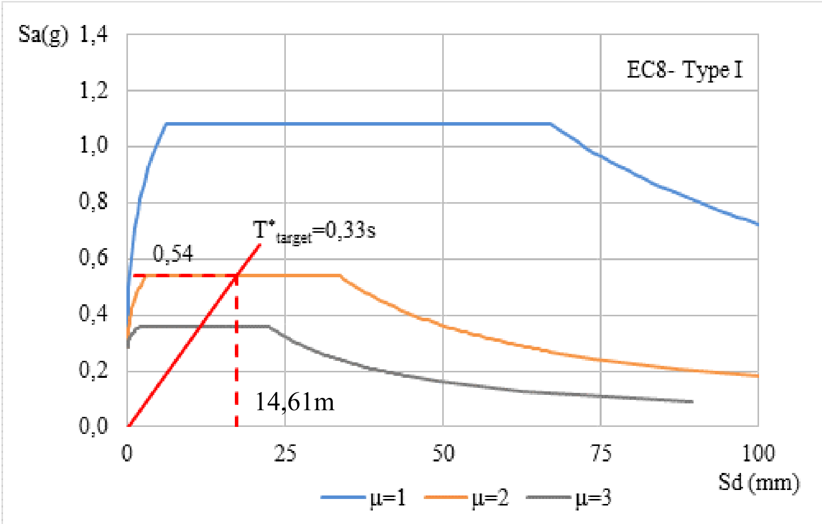

Figure 1: Calculation of the target period of the ESDOF system through ADRS

Table 8: Required stiffness for the correction of the response shape in x-x and y-y direction

Stiffness in x-x direction, K_x (kN)					
Storey	Existing building	Torsionally balanced building (Phase I)	Required Stiffness for target shape (Phase II)	Added stiffness (Design of R.C. jackets)	Stiffness at the end of the retrofit design
1st	87077,1	193352,2	246966,7	49170,8	242523,0
2nd	165381,7	267249,8	296360,0	0,0	267249,8
3rd	127008,9	228877,0	172876,7	0,0	228877,1
Stiffness in y-y direction, K_y (kN)					
Storey	Existing building	Torsionally balanced building (Phase I)	Required Stiffness for target shape (Phase II)	Added stiffness (Design of R.C. jackets)	Stiffness at the end of the retrofit design
1st	96447,9	210207,9	246966,7	43432,2	253660,1
2nd	181295,1	290648,2	296360,0	0,0	290648,2
3rd	137747,3	247100,3	172876,7	0,0	247100,3

The target stiffness of the ESDOF system (K^*) is defined from:

$$K^* = 4 \cdot \pi^2 \frac{M^*}{T^2_{target}} = 83666,26 kN/m \tag{19}$$

The stiffness distribution along the height of the building is estimated according to Eqs. (9), (10):

$$K_1 = 246967 kN/m\,;\; K_2 = \frac{w_2}{w_1} \cdot K_1 = 296360 kN/m\,;\; K_3 = \frac{w_3}{w_1} \cdot K_1 = 172877 kN/m$$

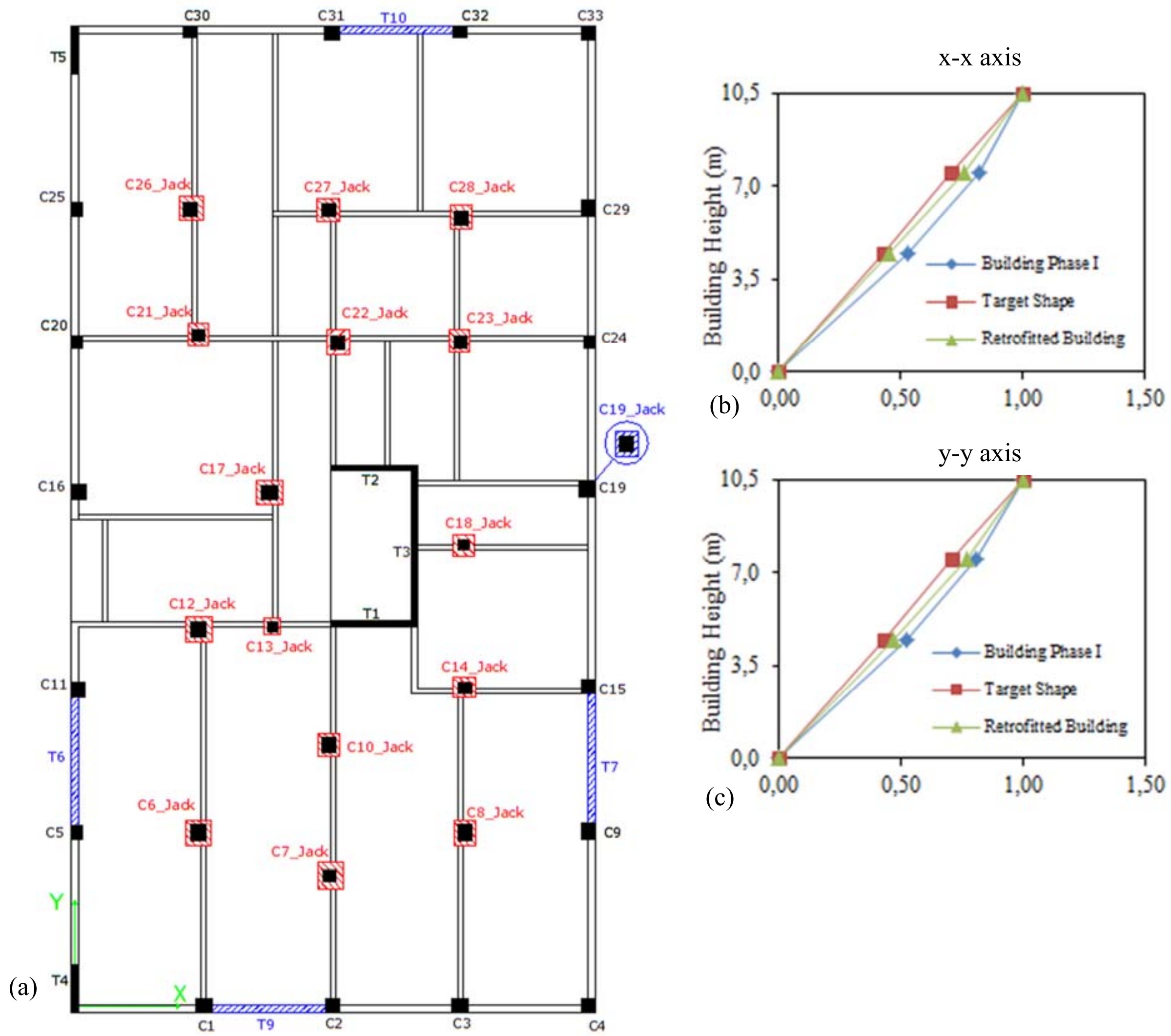

Figure 13: (a) Retrofit solution according to the proposed methodology; Phase I: Elimination of torsional effects through the addition of the blue colored members at the perimeter of the building; Phase II: Strengthening for a target response shape through strengthening of the red colored vertical members. Response Shape of the retrofitted structure according to Rayleigh Method (b) along x-x axis (c) y-y axis.

Table 8 presents information related to the stiffness of the building at each design phase. The required stiffness distribution along the height of the building for the target response shape is also presented. It is observed that only in the first and second floor stiffness addition is required, whereas in the third floor the stiffness of the existing building after design phase I is already higher than the required stiffness for the target response shape. The latter implies that even in the case that the stiffness in the first and second storey are increased as to comply with the stiffness corresponding to the target response, the resulting lateral response shape would slightly deviate from the target one. It was decided to modify only the stiffness of the first storey by the addition of R.C. jackets (i.e. longitudinal bars pass through holes drilled in the slab and anchored in the second storey) due to the cost effectiveness of this solution. The columns to be jacketed at the end of the design phase II are depicted by red colour in Fig. 13(a). The selection of this specific group of columns and the distribution of the target added stiffness along them did not affect the center of stiffness as defined in design phase I. Details regarding dimensioning of the R.C. jacketed members appear in Table 9. The proposed retrofit solution may lead to a lateral response shape very close to the target one as seen in Fig. 13(b), (c) after applying the Rayleigh iterative method.

Table 9: Reinforcement details of R.C. jacketed members

R.C. Jacketed Columns									
	b_x (m)	b_y (m)	Long. Reinforcement (mm)	Stirrups (mm)	ρ_{itot} (%)	K_x (kN/m)	K_y (kN/m)	ΔK_x (kN/m)	ΔK_y (kN/m)
C21	0,45	0,40	8Ø20	Ø14/100	1,40%	4377,2	3555,5	3076,3	2254,7
C22	0,50	0,45	8Ø22	Ø14/100	1,35%	6347,5	5285,1	4012,4	2950,0
C23	0,45	0,45	8Ø22	Ø14/100	1,50%	5043,7	5043,7	3847,1	3847,1
C18	0,45	0,40	8Ø22	Ø14/100	1,53%	4785,8	3882,7	3692,5	3146,0
C14	0,50	0,50	8Ø22	Ø14/100	1,22%	6322,8	6322,8	4307,1	4858,6
C10	0,50	0,45	8Ø18	Ø14/100	0,90%	4886,7	4076,6	2721,9	1911,8
C12	0,55	0,48	8Ø22	Ø14/100	1,16%	8358,5	6508,9	4253,8	2404,2
C17	0,50	0,45	8Ø16	Ø14/100	0,71%	4321,1	3608,0	985,7	1050,0
C13	0,35	0,35	8Ø22	Ø14/100	1,95%	2847,5	2847,5	2376,1	2376,1
C6	0,55	0,50	8Ø22	Ø16/100	1,11%	8436,6	7177,3	4312,2	3052,9
C7	0,45	0,45	8Ø18	Ø14/100	1,01%	3846,5	3846,5	2653,0	2653,0
C8	0,50	0,50	8Ø22	Ø14/100	1,22%	6510,5	6510,5	3941,9	3162,4
C26	0,45	0,45	8Ø22	Ø14/100	1,50%	5172,4	5172,4	2880,5	2880,5
C27	0,45	0,45	8Ø22	Ø14/100	1,50%	6003,1	6003,1	3155,3	3929,9
C28	0,50	0,50	8Ø18	Ø14/100	0,81%	5655,0	5655,0	2955,0	2955,0

3.4 Assessment of the retrofitted structure

3.4.1 Eigenvalue Analysis

Eigenvalue analysis was performed to the retrofitted structure as to verify the results conducted by hand calculations. The modal response parameters are presented in Table 10, whereas the first three modes are shown in Fig. 14. It is observed that first and second mode are translational with mass participation over 80%. Moreover, the fundamental period (0.35s) is close to the target one (0.33s).

Table 3: Modal response parameters of the retrofitted building

No.	Period (s)	Modal participation mass ratio		
		Ux	Uy	Rz
1	0,350	80,13%	0,00%	0,09%
2	0,258	0,01%	80,44%	0,13%
3	0,235	0,12%	0,14%	79,37%

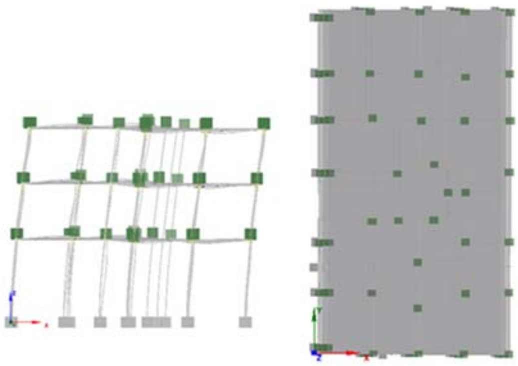

(a) **1st mode**: T1=0,350s MPRM=80,13%

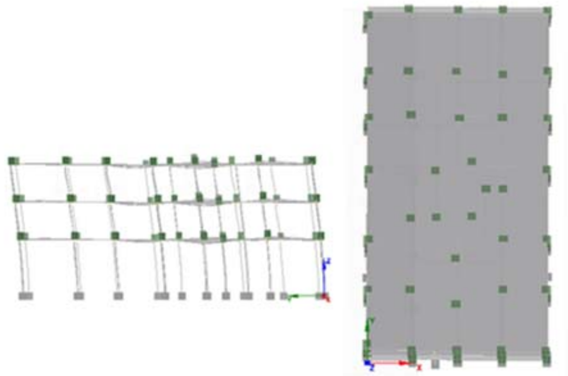

(b) **2nd mode**: T_2=0,258s MPRM=80,44%

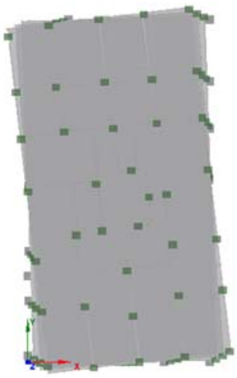

(c) **3rd mode**: T_3=0,235s MPRM=79,37%

Figure 2: Deformed shape, periods and modal participating mass ratio (MPMR) of the retrofitted building: (a) 1st mode; (b) 2nd mode; (c) 3rd mode

3.4.2 Pushover Analysis

Nonlinear static analyses were carried out for the modal and the uniform pattern. The response curve after application of the uniform distribution along the height of the building of the applied lateral load is presented in Fig. 15 along with the response curve of the existing building for the same pattern in the x-x and y-y directions (The blue dot placed on the curve of the existing building corresponds to the point of failure). As it is observed the retrofitted building has increased substantially its strength.

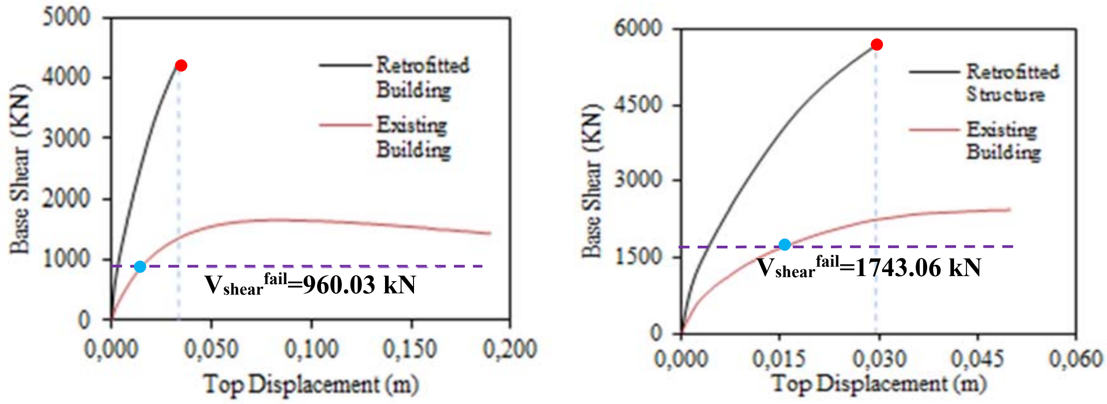

Figure 15: Pushover curves for the existing and the retrofitted building along (a) x-x and (b) y-y axis

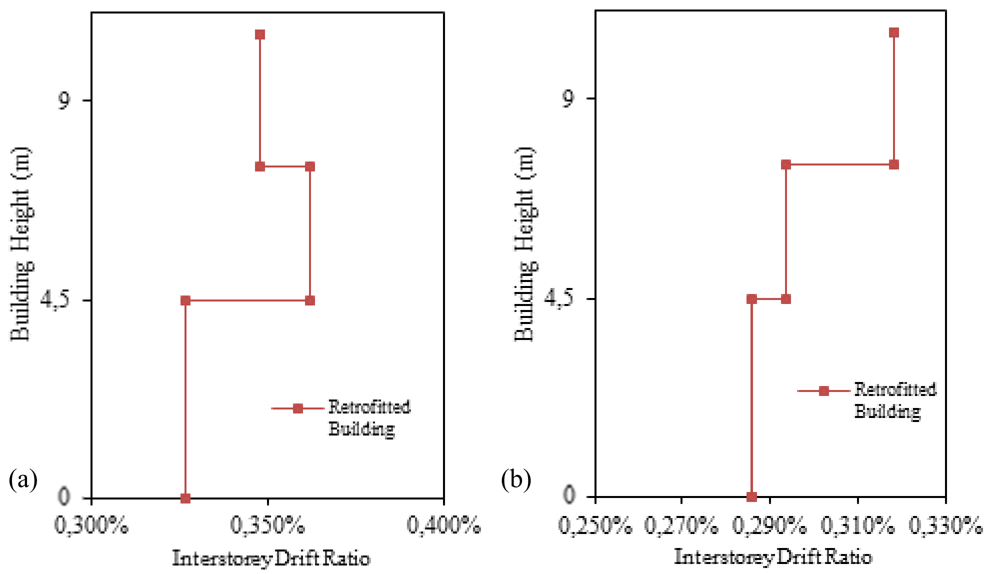

Figure 16: Interstorey drift ratio of the retrofitted and the existing building along (a) x-x and (b) y-y axis

The interstorey drift profiles that correspond to the maximum top displacement of the retrofitted building (red dot in Fig. 15) in x-x and y-y axis are presented in Fig. 16. Moreover, the lateral response shape at the maximum roof displacement is compared to the triangular response shape in Fig. 17.

The proposed retrofit solution manages to keep almost a uniform distribution of interstorey drift along the building height even in the post-yield region. Deviations from the target response shape are justified and expected in the sense that one has to deal with existing buildings which after elimination of torsional sensitivity (design phase I) have a pre-defined distribution of stiffness along the height of the building that may impose limitations when compared to the desirable distribution of stiffness along the height of the building as to comply with the target response shape.

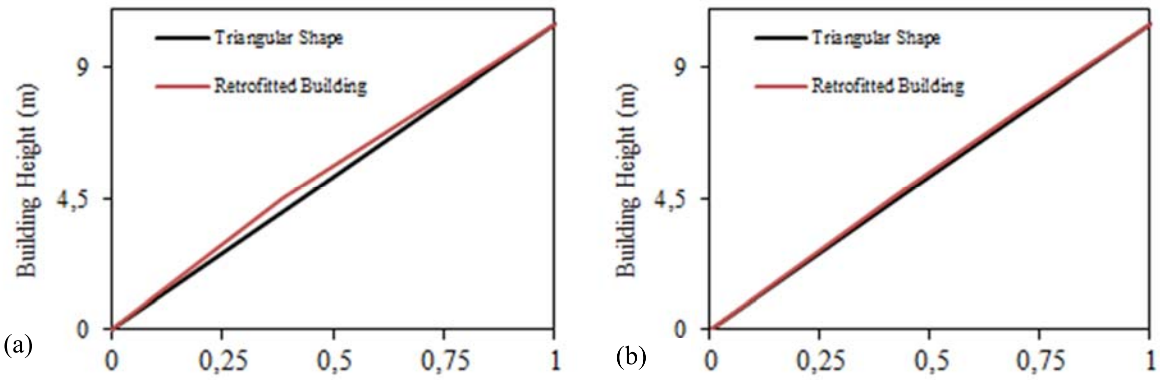

Figure 17: Comparison of the target response shape and the lateral response shape of the retrofitted building along (a) x-x (b) y-y axis

4 CONCLUSIONS

A retrofit design methodology for the seismic upgrading of rotationally sensitive existing R.C. buildings was presented. The proposed methodology aims to modify substantially the response by minimizing structural eccentricities and simultaneously increasing torsional resistance and stiffness. For this purpose, stiffness is added through the adoption of global intervention methods at the periphery of the building so as to provide a building symmetric in plan and torsionally balanced. The lateral response shape in the two orthogonal axes (x-x and y-y) is further modified as to comply with the target response shape. This is achieved by a weighted distribution of additional stiffness along the height of the building. The proposed methodology was implemented to a three-storey building constructed in the early 1970s in North Greece. The validity of the proposed methodology was assessed by carrying out inelastic analyses with the use of a three-dimensional finite element model of the retrofitted structure. The results indicate the efficiency of the proposed design methodology for the seismic upgrading of existing torsionally unbalanced R.C. buildings.

REFERENCES

[1] G.E Thermou, A.S. Elnashai, Seismic retrofit schemes for R.C. structures and local-global consequences. *Journal of Progress in Structural Engineering and Materials*, Wiley InterScience, **8(1)**, 1-15, 2006.

[2] G.E. Thermou, S.J. Pantazopoulou, A.S. Elnashai, Design methodology for seismic upgrading of substandard R.C. structures. Journal of Earthquake Engineering, **4(1)**, 582-606, 2007.

[3] S.J. Pardalopoulos, S. J. Pantazopoulou, Spatial component analysis of 3-D Displacement and Storey Drift in R.C. Buildings Under Seismic Loads. Computational Methods in Earthquake Engineering, (Ed.: M. Papadrakakis et al.), 123-145, 2010. Series: Computational Methods in Applied Sciences 21, DOI 10.1007/978-94-007-0053-6_6, Springer Publishers.

[4] G.E. Thermou, S.J. Pantazopoulou, A.S. Elnashai, Upgrading of R.C. structures for a target response shape. *Thirteenth World Conference on Earthquake Engineering*, Vancouver, Canada, Paper No 1412, 2004.

[5] G.E. Thermou, S.J. Pantazopoulou, A.S. Elnashai, Design methodology for seismic upgrading of existing R.C. structures. *fib Symposium* “Keep Concrete Attractive”, Budapest, Hungary, Paper No 302, 2005.

[6] G.E. Thermou, A.S. Elnashai, S.J. Pantazopoulou, Retrofit Yield Spectra–a practical device in seismic rehabilitation. *Earthquake and Structures*, **3(2)**, 141-168, 2012.

[7] G.E. Thermou, S.J. Pantazopoulou, A.S. Elnashai, Global interventions for seismic upgrading of substandard R.C. buildings. *Journal of Structural Engineering*, ASCE, **138(3)**, 387-401, 2012.

[8] M.A. Aschheim, E.F. Black, Yield Point Spectra for seismic design and rehabilitation. *Earthquake Spectra*, EERI, **16(2)**, 317-336, 2000.

[9] Royal Decree, Seismic design of reinforced concrete buildings. Royal Decree (19/26.02.1959), Ministry of Public Works, Greece (in Greek), 1959.

[10] Eurocode 8, Design of structures for earthquake resistance - Part I: General rules, seismic actions and rules for buildings. EN1998-1-2004:E, European Committee for Standardization (CEN), Brussels, 2004.

[11] Eurocode 8, Design of structures for earthquake resistance. Part III: Assessment and retrofitting of buildings. EN 1998-3:2005(E), European Committee for Standardization (CEN), Brussels, 2005.

[12] Greek Code for Interventions (KANEPE). *Earthquake Planning and Protection Organization*, Athens, 2013.

[13] H. Krawinkler, G.D.P.K. Seneviratna, Pros and cons of a pushover analysis of seismic performance evaluation. *Engineering Structures*, **20(4-6)**, 452-464, 1998.

[14] S. Kim, E. D'Amore, Push-over analysis procedure in earthquake engineering. *Earthquake Spectra*, **15(3)**, 417-434, 1999.